Crystal Structure of the Caged Magnetic Compound DyFe2Zn20 at Low Temperature Magnetic Ordering State

	Kishii Nobuya, Tateno Shota, Ohashi Masashi, Isikawa Yosikazu
journal or publication title	Physics Procedia
volume	75
page range	664-670
year	2015-12-01
URL	http://hdl.handle.net/2297/45892

Crystal structure of the caged magnetic compound DyFe$_2$Zn$_{20}$ at low temperature magnetic ordering state

Nobuya Kishii[1], Shota Tateno[1], Masashi Ohashi[2] and Yosikazu Isikawa[3]

[1] Graduate School of Natural Science and Technology, Kanazawa University ,Kakuma-machi, Kanazawa, 920-1192, Japan

[2] Institute of Science and Engineering, Kanazawa University,Kakuma-machi, Kanazawa, 920-1192, Japan
ohashi@se.kanazawa-u.ac.jp

[3] Graduate School of Science and Engineering, University of Toyama, Gofoku, Toyama, 930-8555, Japan
isikawa@sci.u-toyama.ac.jp

Abstract

We have carried out X-ray powder diffraction and thermal expansion measurements of the caged magnetic compound DyFe$_2$Zn$_{20}$. Even though a strong magnetic anisotropy exists in the magnetization and magnetic susceptibility due to strong exchange interaction between Fe and Dy, almost all X-ray powder diffraction peaks at 14 K correspond to Bragg reflections of the cubic structural models not only at room temperature paramagnetic state but also at low temperature magnetic ordering state. Although the temperature change of the lattice constant is isotropic, an anomalous behavior was observed in the thermal expansion coefficient around 15 K, while the anomaly around $T_\mathrm{C} = 53$ K is not clear. The results indicate that the volume change is not caused by the ferromagnetic interaction between Fe and Dy but by the exchange interaction between two Dy ions.

1 Introduction

The series of cubic RT$_2$Zn$_{20}$ compounds has been recently closely examined, where R is a rare earth atom and T is a transition metal [1, 2, 3, 4, 5, 6, 7]. In these compounds, R occupies the 8a site surrounded by 16 Zn atoms, and T occupies the 16d site surrounded by 12 Zn atoms. The exchange interaction between two R atoms is weak, because the R atoms are diluted in this compound. In fact, in the case of T = Co or Ru, the Curie temperature T_C is less than 10 K for any R. However, in the case of the Fe series, T_C is significantly enhanced. It has been hypothesized that the magnetism of Fe atoms is involved in this high T_C.

DyFe$_2$Zn$_{20}$ is ferromagnetic at temperatures below $T_\mathrm{C} = 45$ or 53 K [1, 2]. Below T_C, the ^{57}Fe Mössbauer spectrum of DyFe$_2$Zn$_{20}$ has a complicated shape compared with that of nonmagnetic YFe$_2$Zn$_{20}$ [3]. These results indicate that the small magnetic moments of Fe atoms interact antiferromagnetically with those of the Dy atoms. Isikawa et al. examined magnetization, magnetic susceptibility and specific heat of DyFe$_2$Zn$_{20}$ single crystals, and found experimentally unusual magnetic anisotropies, i.e. a large magneto-crystalline anisotropy at 2 K and a metamagnetic transition in the field along the [100] direction, which disappears at temperatures above 30 K below T_C [2]. It is indicated that the exchange interaction between Dy and Fe atoms in DyFe$_2$Zn$_{20}$ is the cause of the ferromagnetism in this compound, and that the higher T_C of DyFe$_2$Zn$_{20}$ compared with that of DyRu$_2$Zn$_{20}$ as well as the large magneto-crystalline anisotropy is caused by this exchange interaction. The magnetic moments of Dy

and Fe atoms at 0 K are found to be 10 μ_B/Dy and 0.2 μ_B/Fe, respectively, which is in good agreement with the values estimated by the ^{57}Fe Mössbauer spectroscopy [3].

In general, large magneto-crystalline anisotropy is caused in compounds with low structural symmetry [8, 9], and some magnetic compounds show a change in lattice parameters and thermal expansion at magnetic or superconducting transition temperatures [10, 11, 12]. Some caged magnetic compounds RT_2Zn_{20} are also expected to have a lower structural symmetry. In $LaRu_2Zn_{20}$, $CeRu_2Zn_{20}$, $PrRu_2Zn_{20}$, and $LaIr_2Zn_{20}$, the anomalies have been observed in the temperature dependence of magnetic susceptibility, heat capacity and electrical resistivity at approximately 150, 130, 138, and 200 K, respectively [4, 5]. However, their crystal structure are not sufficiently clear. As for $PrRh_2Zn_{20}$, although the anisotropic magnetic field-temperature phase diagram is determined for the antiferroquadrupolar ordering transition at low temperatures [6], the crystallographic phase transition of $PrRh_2Zn_{20}$ near 140 K is speculated to be a transition of the site symmetry of R atoms from T_d to T, with keeping the cubic symmetry [7].

The large magnetic anisotropy of $DyFe_2Zn_{20}$ may also cause a reduction in the structural symmetry at the low temperature magnetic phase. However, it is not clear even whether the cubic symmetry is kept or not. In this study, we performed X-ray powder diffraction and thermal expansion measurements to clarify the crystallographic symmetry of $DyFe_2Zn_{20}$ at the wide temperature range between the magnetic ordering state at low temperature and the paramagnetic state at room temperature.

2   Experimental Procedure

Single crystals of $DyFe_2Zn_{20}$ were grown by the Zn self-flux method. The $DyFe_2Zn_{20}$ crystals were obtained as follows: the elements were placed in an alumina crucible at a ratio Dy: Fe: Zn = 1: 2: 40. The system was then sealed in a quartz tube under 0.33 atm argon gas. The sample was placed in an electric furnace and heated to 1050 °C, where it remained at constant temperature for 0.5 h. The temperature was then lowered to 800 °C. After maintaining this temperature for 10 h, the sample temperature was then lowered to 500 °C at a rate of 3 °C/h. Excess Zn was separated and removed by centrifugation.

X-ray diffraction patterns were obtained using a Rigaku X-ray diffractometer, RINT 2500, with a graphite counter monochromator and an X-ray generator with a rotating Cu anode. The generator was operated at 50 kV and 300 mA. For the X-ray diffraction measurements, the crystal was crushed and powdered using a mortar and pestle. A platelike powder sample was mounted on a copper sample holder. The sample was fixed in a closed-cycle He gas refrigerator mounted on the diffractometer. The sample was cooled from room temperature to 14 K. Diffraction patterns between 15° and 120° were measured at a scanning speed of $2\theta = 0.02°$/min. Data were collected at every $2\theta = 0.008°$. The diffraction patterns were analyzed by the Rietveld method to obtain accurate lattice parameters using computer program RIETAN-2000 [13]; calculations were carried out by a conjugate direction method.

Thermal expansion was measured by means of strain gauge method [12], in which two gages were used as an active (sample) and a dummy (reference) gauge. A commercial physical property measurement system (PPMS, Quantum Design Co. Ltd.) is combined with a compact bridge-circuit box to measure the extremely small resistance changes of the strain gauge [14]. Here, the strain gauges are glued along the [100] and [111] directions of $DyFe_2Zn_{20}$ single crystal. Cu (6N) was used as a reference material.
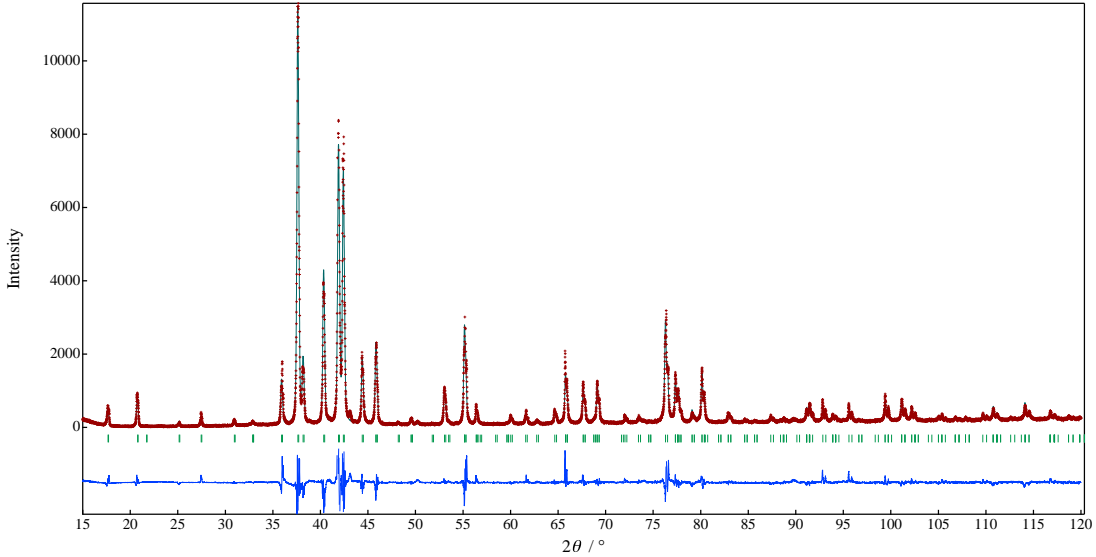
2

Figure 1: Experimental (red symbols) and refined (red solid curve) X-ray powder diffraction pattern of $DyFe_2Zn_{20}$ at 300 K. The vertical marks correspond to 2θ Bragg positions. The lower blue curve is the difference diagram.

3   Results and discussion

3.1   X-ray diffraction

The X-ray powder diffraction pattern of $DyFe_2Zn_{20}$ at 300 K is shown in Figure 1. The upper symbols illustrate the observed data (red symbols). Although small impurity peaks are observed at $2\theta = 43.10°$ and $50.10°$, almost all peaks correspond to Bragg reflections of the cubic structural model as shown in the vertical marks. Here, we assumed that $DyFe_2Zn_{20}$ crystalizes in a cubic $CeCr_2Al_{20}$ type structure (space group $Fd\bar{3}m$, No. 227), and analyzed the diffraction pattern by the Riedveld method. The calculated pattern and the difference diagram are illustrated in Figure 1 as green and blue solid curve, respectively. The lattice parameter is obtained to be $a = 14.09183 \pm 0.00007$ Å, which is closed to the one reported previously [1]. Since the reliability factors are relatively large ($R_{WP} = 13.03\%$, $R_p = 9.67\%$, $R_R = 17.39$ %, $R_e = 13.03\%$, and $s = 2.1658\%$), more precise experiments are planed to determine the space group and all other structural parameters accurately.

Figures 2 and 3 show the X-ray powder diffraction pattern of $DyFe_2Zn_{20}$ at 30 and 14 K, respectively. It is found that both patterns are almost similar to that at 300K, that is, new peaks do not appear within the experimental error even when decreasing temperature. It means that structure phase transformation does not exist at any magnetic transition temperature. The data is analyzed by the Rietveld profile method and the lattice parameter is obtained to be $a = 14.03483 \pm 0.00006$ Å and 14.03444 ± 0.00006 Å at 30 and 14 K, respectively.
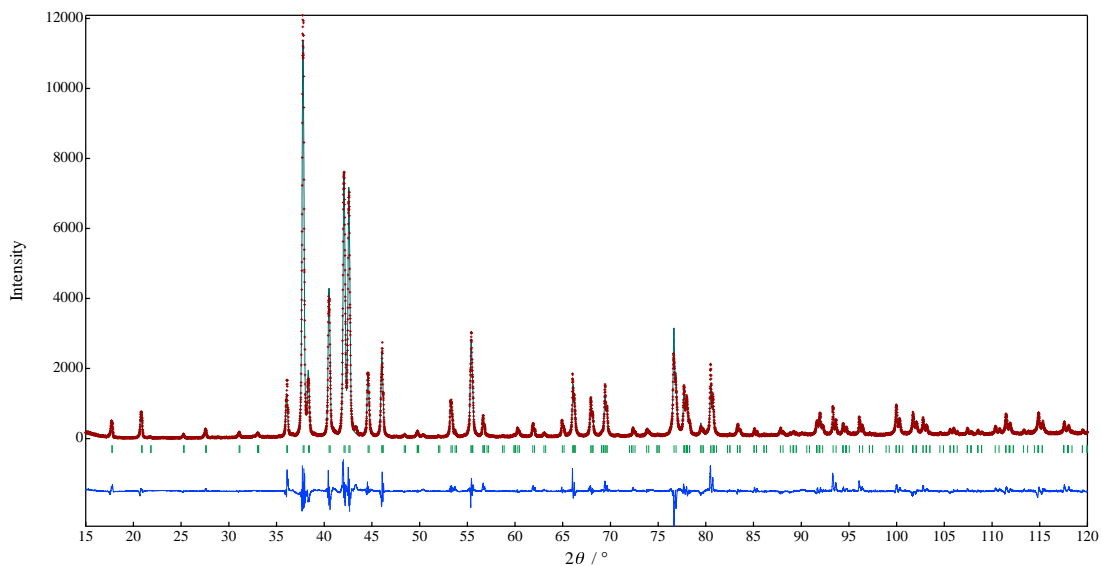
Figure 2: Experimental and refined X-ray powder diffraction pattern of DyFe$_2$Zn$_{20}$ at 30 K. The vertical marks correspond to 2θ Bragg positions.
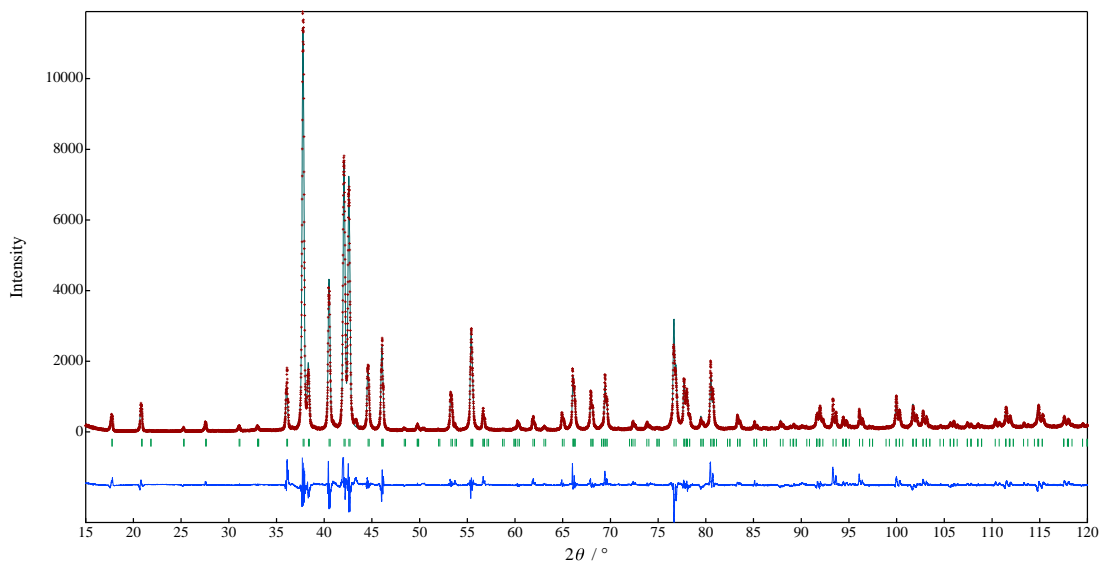

Figure 3: Experimental and refined X-ray powder diffraction pattern of DyFe$_2$Zn$_{20}$ at 14 K. The vertical marks correspond to 2θ Bragg positions.

4
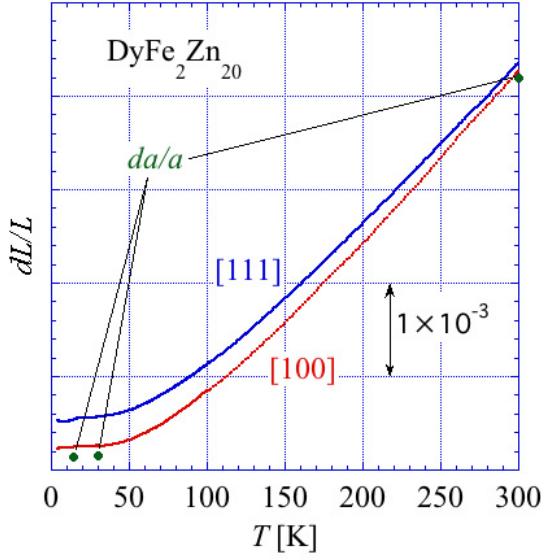
Figure 4: The linear thermal expansion dL/L (left flame) of $DyFe_2Zn_{20}$ as a function of temperature along [100] and [111] directions. The change of the lattice constant da/a, which is estimated from the result of the X-ray diffraction pattern, is also plotted.

3.2   Thermal expansion

Figure 4 shows the temperature dependence of the linear thermal expansion dL/L along [100] and [111] directions of $DyFe_2Zn_{20}$ single crystal. It is seen that both dL/L decrease linearly with decreasing temperature, and tend to saturates below 50 K. For comparison, we plotted the change of the lattice constant da/a, which is obtained from the X-ray diffraction pattern in Figures 1, 2 and 3. It is in good agreement with that obtained by the result of the measurement of the thermal expansion.

Figure 5 shows the temperature dependence of the linear thermal expansion coefficient $\alpha(T)$ along [100] and [111] directions of $DyFe_2Zn_{20}$. Here, $\alpha(T)$ is defined as the derivative of dL/L with respect to temperature. A sharp peak is found in both $\alpha(T)$ curves along both [100] and [111] directions at approximately 15 K while the anomaly around T_C is not clear. Similar behavior is reported in the result of the specific heat, where a broad peak is observed at 15 K. Moreover, the strong anisotropy of the magnetization is also observed below 20 K due to the exchange interaction between two Dy ions.

Such behavior has been analyzed based on the crystal electric field, Zeeman energy, an usual exchange interaction n_{RR} between two Dy atoms, and the strong exchange interaction n_{FeR}[2]. n_{FeR} is 80 times larger in magnitude than n_{RR} in $DyFe_2Zn_{20}$. Thus, T_C is enhanced by this n_{FeR} while the strong anisotropy of the magnetization below 20 K is related to the small n_{RR}. On the other hand n_{RR} is caused by the distance between Dy ions in $DyFe_2Zn_{20}$, while n_{FeR} is presumably due to large overlapping of the wave function between the itinerant $3d$ and the localized $4f$ electrons. Thus, it is reasonable to assume that n_{RR} is sensitive to volume change of $DyFe_2Zn_{20}$ compared with n_{FeR}. This hypothesis is consistent with the fact that a sharp peak is found around 15 K.

On the other hand, both $\alpha(T)$ are almost same within the experimental error, indicating that
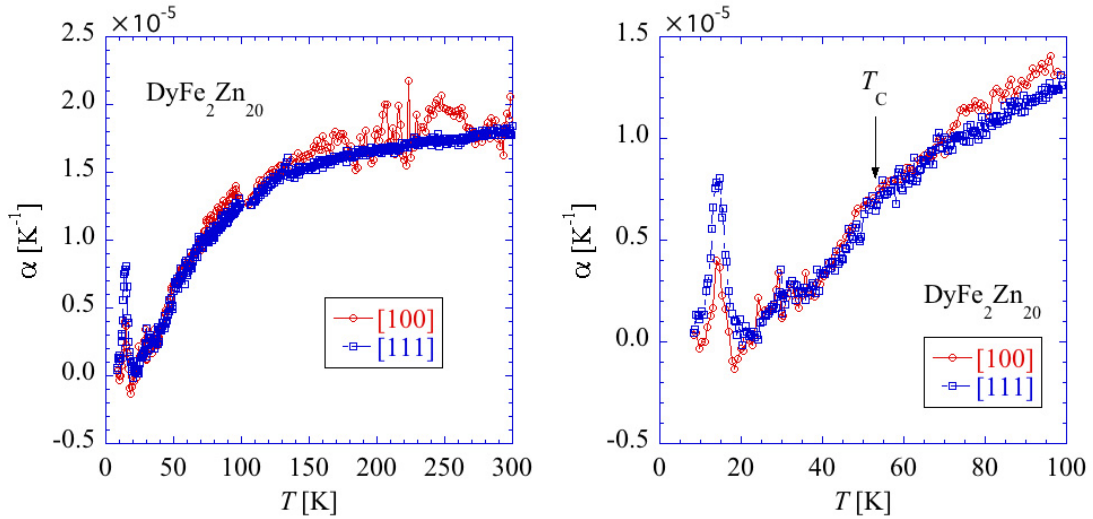
Figure 5: The thermal expansion coefficient α of $DyFe_2Zn_{20}$ as a function of temperature along [100] and [111] directions. $T_C = 53$ K is determined by the magnetization measurement [2].

the volume change is isotropic and that n_{RR} is not related to any structural phase transformation in $DyFe_2Zn_{20}$. This is in contrast to the case of $DyAl_2$, where the ferromagnetic transition causes low structural symmetry from cubic to tetragonal structure due to a large magnetic anisotropy below $T_C = 62$ K [14, 15]. This difference may be attributed to a difference in the magnitude of the exchange interaction in each compounds, that is, in the case of $DyFe_2Zn_{20}$, the distance between Dy atoms is relatively large and n_{RR} is extremely small in magnitude than n_{FeR} in $DyFe_2Zn_{20}$, while a ferromagnetic ordering of $DyAl_2$ is mainly caused by local magnetic moments of Dy ions.

4   Conclusions

The accurate study of $DyFe_2Zn_{20}$ by X-ray powder diffraction measurements suggests that $DyFe_2Zn_{20}$ crystalizes in a cubic $CeCr_2Al_{20}$ type structure not only at room temperature paramagnetic state but also at low temperature magnetic ordering state. No structural phase transformation is caused by the magnetic phase transition, and the temperature change of the lattice constant is isotropic. However, an anomalous behavior was observed in the thermal expansion coefficient around 15 K, while the anomaly around T_C is not clear. Compared with the results of the magnetization and the specific heat in the previous reports, it is reasonable to assume that the volume change is mainly caused by the exchange interaction between two Dy ions.

Acknowledgments

References

[1] Jia S Ni N Bud'ko S L and Canfield P C. Magnetic properties of RFe_2Zn_{20} and RCo_2Zn_{20} (R= Y, Nd, Sm, Gd-Lu). *Phys. Rev. B*, 80:104403–1–17, 2009.

[2] Isikawa Y Mizushima T Miyamoto S Kumagai K Nakahara M Okuyama H Tayama T Kuwai T Lejay P. Enhancement of curie temperature due to the coupling between Fe itinerant electrons and Dy localized electrons in $DyFe_2Zn_{20}$. *J. Korean Phys. Soc.*, 63:644–1–5, 2013.

[3] Tamura I Isikawa Y Mizushima T and Miyamoto S. Study of ^{57}Fe Mössbauer effect on $DyFe_2Zn_{20}$ and YFe_2Zn_{20}. *J. Phys. Soc. Jpn*, 82:114703–1–4, 2013.

[4] Isikawa Y Mizushima T Kumagai K and Kuwai T. Dense kondo effect in caged compond $CeRu_2Zn_{20}$. *J. Phys. Soc. Jpn*, 82:083711–1–4, 2013.

[5] Onimaru T Matsumoto K T Inoue Y F Umeo K Saiga Y Matsushita Y Tamura R Nishimoto K Ishii I Suzuki T and Takabatake T. Superconductivity and structural phase transitions in caged compounds RT_2Zn_{20} (R = La, Pr, T = Ru, Ir). *J. Phys. Soc. Jpn*, 79:033704–1–4, 2010.

[6] Ishii I Muneshige H Kamikawa S Fujita T K Onimaru T Nagasawa N Takabatake T and Suzuki T. Antiferroquadrupolar ordering and magnetic-field-induced phase transition in the cage compound $PrRh_2Zn_{20}$. *Phys. Rev. B*, 87:205106–1–7, 2013.

[7] Iwasa K Kobayashi H Onimaru T Matsumoto K T Nagasawa N Takabatake T Kawamura S O Kikuchi T Inamura Y and Nakajima K. Well-defined crystal field splitting schemes and non-kramers doublet ground states of f electrons in PrT_2Zn_{20} (T = Ir, Rh, and Ru). *J. Phys. Soc. Jpn.*, 82:043707–1–4, 2013.

[8] Cho B K Ohashi M, Oomi G and Canfield P C. Magnetotransport in the magnetic-superconductor $HoNi_2B_2C$. *Physica Status Solidi B*, 247:599–601, 2010.

[9] Ohashi M Oomi G and Satoh I. Ac magnetic susceptibility studies of single crystalline $CeNiGe_2$ under high pressure. *J. Phys. Soc. Jpn.*, 76:114712–1–3, 2007.

[10] Fujishita F Hayashi Y Saito M Unno H Kaneko H Okamoto H Ohashi M Kobayashi Y Sato M. X-ray diffraction study of spontaneous strain in Fe-pnictide superconductor, $NdFeAsO_{0.89}F_{0.11}$. *Eur. Phys. J. B*, 85:52–1–6, 2012.

[11] Oishi T Ohashi M Suzuki H and Satoh I. The negative volume magnetostriction of $GdAl_2$ with a cubic laves structure. *Journal of Physics: Conference Series*, 200:082022–1–4, 2010.

[12] Ohashi M Tashiro A Oomi G Maeda E Zheng X G. Effect of pressure on the magnetic phase transition in cupric oxide. *Phys. Rev. B*, 73:134421–1–6, 2006.

[13] Izumi F and Ikeda T. A Rietveld-analysis program rietan-98 and its applications to zeolites. *Mater. Sci. Forum*, 321-324:198–204, 2000.

[14] Tateno S Kishii N and Ohashi M. A new bridge circuit-type detector to measure precise resistance change of strain gauge at low temperature and magnetic field. Submitted for publication to Physics Procedia, 2015.

[15] Buschow K H J. Rare earth compounds. *Ferromagnetic Materials*, 1:297–414, 1980.